Since January 2020 Elsevier has created a COVID-19 resource centre with free information in English and Mandarin on the novel coronavirus COVID-19. The COVID-19 resource centre is hosted on Elsevier Connect, the company's public news and information website.

Journal of Hazardous Materials 425 (2022) 128051

Contents lists available at ScienceDirect

Journal of Hazardous Materials

journal homepage: www.elsevier.com/locate/jhazmat

Research Paper

Predominant airborne transmission and insignificant fomite transmission of SARS-CoV-2 in a two-bus COVID-19 outbreak originating from the same pre-symptomatic index case

Pan Cheng [a,1], Kaiwei Luo [b,1], Shenglan Xiao [a,c,1], Hongyu Yang [d], Jian Hang [d], Cuiyun Ou [d], Benjamin J. Cowling [e], Hui-Ling Yen [e], David SC Hui [f], Shixiong Hu [b], Yuguo Li [a,e,*]

[a] Department of Mechanical Engineering, The University of Hong Kong, Hong Kong, China
[b] Hunan Provincial Center for Disease Control and Prevention, Changsha, China
[c] School of Public Health, Sun Yat-sen University, Guangzhou, China
[d] School of Atmospheric Sciences, Sun Yat-sen University, and Southern Marine Science and Engineering Guangdong Laboratory (Zhuhai), Zhuhai, China
[e] School of Public Health, The University of Hong Kong, Hong Kong, China
[f] Department of Medicine and Therapeutics, The Chinese University of Hong Kong, Hong Kong, China

ARTICLE INFO

Editor: Dr. Danmeng Shuai

Keywords:
Airborne transmission
Fomite transmission
Quanta generation rate
COVID-19

ABSTRACT

The number of people infected with severe acute respiratory syndrome coronavirus 2 (SARS-CoV-2) continues to increase worldwide, but despite extensive research, there remains significant uncertainty about the predominant routes of SARS-CoV-2 transmission. We conducted a mechanistic modeling and calculated the exposure dose and infection risk of each passenger in a two-bus COVID-19 outbreak in Hunan province, China. This outbreak originated from a single pre-symptomatic index case. Some human behavioral data related to exposure including boarding and alighting time of some passengers and seating position and mask wearing of all passengers were obtained from the available closed-circuit television images/clips and/or questionnaire survey. Least-squares fitting was performed to explore the effect of effective viral load on transmission risk, and the most likely quanta generation rate was also estimated. This study reveals the leading role of airborne SARS-CoV-2 transmission and negligible role of fomite transmission in a poorly ventilated indoor environment, highlighting the need for more targeted interventions in such environments. The quanta generation rate of the index case differed by a factor of 1.8 on the two buses and transmission occurred in the afternoon of the same day, indicating a time-varying effective viral load within a short period of five hours.

1. Introduction

The coronavirus disease 2019 (COVID-19) pandemic, which is caused by severe acute respiratory syndrome coronavirus 2 (SARS-CoV-2), is continuing worldwide. As of early October 2021, nearly 240 million people had been infected with SARS-CoV-2 and more than 4.8 million people had died from COVID-19 (https://covid19.who.int/). And at least one third of SARS-CoV-2 infections are asymptomatic (Oran and Topol, 2021). Efforts to identify the predominant transmission routes of SARS-CoV-2 are ongoing. During the early phase of the pandemic, the World Health Organization (2020a) recognized that SARS-CoV-2 could be transmitted by direct contact with an infected person or by contact (over short distances) with droplets exhaled by an infected person, but airborne transmission was considered as unlikely. In the July 2020 update, the WHO recognized that airborne and fomite transmission of SARS-CoV-2 might be possible, although there was no direct evidence for this (World Health Organization, 2020b). In their April 2021 update, the WHO emphasized the roles of "small liquid particles" in short- and long-range airborne transmission of SARS-CoV-2, and stated that fomite transmission was possible: "[p]eople may also become infected by touching surfaces that have been contaminated by the virus when touching their eyes, nose or mouth without cleaning their hands." The United States Centers for Disease Control and Prevention (US CDC, 2021) also stated that fomite transmission was possible but that "the risk is generally considered to be low." Our current understanding of SARS-CoV-2 transmission based on the first 16–17 months of

* Correspondence to: Department of Mechanical Engineering, The University of Hong Kong, Pokfulam, Hong Kong, China.
E-mail address: liyg@hku.hk (Y. Li).
[1] Cheng, Luo, and Xiao contributed equally to this paper.

https://doi.org/10.1016/j.jhazmat.2021.128051
Received 21 October 2021; Received in revised form 6 December 2021; Accepted 7 December 2021
Available online 9 December 2021

the COVID-19 pandemic suggests that evidence is needed to determine the relative importance of the routes of transmission. This information is essential for making evidence-based recommendation on effective non-pharmaceutical interventions to minimize transmission.

The airborne transmission of respiratory viruses involves the expiration of fine virus-laden droplets from an infected person and their subsequent inhalation by a susceptible person. In contrast, fomite transmission is the transfer of surface-borne virus-laden respiratory droplets to a susceptible person; this typically occurs when a person touches a surface bearing virus-laden droplets with his/her hand, and subsequently touches his/her exterior mucosa (e.g., eyes, nose, or mouth) with the same hand, resulting in self-inoculation. Fomite transmission of SARS-CoV-2 was first suspected following the reported survival ability of SARS-CoV-2 on common surfaces (Chin et al., 2020; Van Doremalen et al., 2020). A subsequent experiment in golden hamsters revealed that airborne transmission was more common than fomite transmission (Sia et al., 2020). Nevertheless, scientific and policy debates continue on the relative importance of long-range airborne and fomite routes in SARS-CoV-2 transmission (Li et al., 2021a; Morawska and Cao, 2020; Meselson, 2020).

Two types of data are essential for quantifying the transmission risk of respiratory viruses in indoor spaces. First, data are required on the ventilation rate in the indoor space at the time of exposure. However, a lack of accessibility typically hinders measurement of the ventilation rate at a venue where infection occurred, and such rates have not been reported in most of the published studies of COVID-19 outbreaks (e.g., Bae et al., 2020; Charlotte, 2020; Miller et al., 2021). Second, data are required on human behavior in the indoor space at the time of infection. However, obtaining these data is even more challenging than obtaining ventilation data. Although recordings of closed-circuit television (CCTV) cameras might be available, privacy concerns deter space owners from sharing these recordings. To the best of our knowledge, a restaurant outbreak in Guangzhou, China, is the only outbreak for which both ventilation rate data and human behavior data have been reported (Li et al., 2021b; Zhang et al., 2021). Zhang et al. (2021) obtained data of close contact between people and surface-touching by people for each second, and their analysis revealed little evidence of close-contact and surface-touch transmission in this outbreak.

Another COVID-19 outbreak occurred in January 2020 in Hunan province, China, and was caused by an infected 24-year-old male who traveled successively on two buses, B1 (47 people) and B2 (18 people), in the same afternoon. Ou et al. (2022) measured the ventilation rates on these two buses using a tracer-concentration decay method while the buses were being driven on the same routes (by the same drivers) they had taken on the day of the outbreak. Ten passengers were found to be infected during this outbreak: seven people (including one asymptomatic person) on B1 and two people on B2 when the index case was present, and one person on the return trip of B1 when the index case was not present. Thus, the attack rate was higher on B1 than on B2. The time-averaged ventilation rate was also lower on B1 (1.7 L/s per person) than on B2 (3.2 L/s per person). It was suggested that airborne transmission had occurred on both buses. There are various indoor spaces where there is a high risk of SARS-CoV-2 transmission, and research has focused on the risk in public transport cabins, such as passenger planes (Bogoch et al., 2020; Oztig and Askin, 2020), trains (Zhao et al., 2020), and buses (Zheng et al., 2020). These studies have mainly examined the association between travel and infection, but the association between cabin environment and transmission remains underreported.

Multi-route mechanistic models have been developed to evaluate the infection exposure and risk for respiratory infection as affected by environmental parameters (e.g. Atkinson and Wein, 2008). Similar models have been successfully applied to investigate outbreaks of respiratory infection such as SARS (Xiao et al., 2017), MERS (Xiao et al., 2018a) and influenza (Xiao et al., 2018b). Here we consider both airborne and fomite transmission routes. The airborne transmission has been mostly modeled using a macroscopic mass balance equation approach by assuming that the airborne viral particles are uniformly distributed in an indoor space. It has been widely used (e.g. Buonanno et al., 2020; Aganovic et al., 2021), however, such an mixing assumption cannot reveal the effect of airflow non-uniformity. Computational fluid dynamics (CFD) has been commonly used to explore the effect of non-uniform air distribution on the infection risk, as done by Ou et al. (2022) for this two-bus outbreak. Only steady state simulations were carried out in Ou et al. (2022). Additionally, one approach for evaluating infection risk due to the fomite route is to use a random discrete-time Markov Chain to quantify the surface transmission process. Such an approach has been evaluated using a small-scale benchtop experiment (Xiao et al., 2018c) and a flight cabin outbreak of norovirus (Lei et al., 2017). The data of the two-bus outbreak reported by Ou et al. (2022) offers an opportunity to perform a mechanistic modeling study of SARS-CoV-2 transmission. We therefore mathematically modeled and compared the risk of each passenger on both buses to infection via the fomite and airborne routes.

2. Methods

2.1. The outbreak

The index case, a 24-year-old male, had symptom onset in the late afternoon on January 22, 2020, after he took two buses successively on this day. Seven days later, on January 29, 2020, he was confirmed to have COVID-19. Contact tracing was performed and ten passengers on the two buses were confirmed to be infected: 7 of the 46 passengers on the first bus (a large bus denoted B1, Fig. 1(a)), 1 passenger on the return trip of the same bus (B1), and 2 of the 16 passengers on the second bus (a minibus denoted B2, Fig. 1(b)). On B1, the bus driver was not infected; on B2, neither the bus driver nor the conductor was infected. The basic information of all patients can be found in Ou et al. (2022). In this study, the infected passenger on the return trip of B1 is not studied. All the infected passengers had symptom onset within 14 days of their trips on these buses. On and around January 22, 2020, there were very few confirmed cases in Hunan province, and thus the infected passengers on these buses were unlikely to have been in contact with other infected people. As a result, the 24-year-old male was believed to be the index case of this outbreak (Ou et al., 2022).

In most reported COVID-19 outbreaks, an index case led to a single outbreak in a single infection venue. In contrast, this Hunan outbreak involved two successive buses (B1 and B2) that the index case traveled on in a single afternoon: his B1 journey took 3 h and 20 min, whereas his B2 journey took 1 h. The index case boarded B2 within 15 min of alighting B1, and he was one of the first five passengers to board B1.

The epidemiological and environmental studies of this two-bus outbreak were conducted by Ou et al. (2022). They carried out detailed measurements of the ventilation rates and the dispersion of expired droplets (using tracer gas as surrogate) on the same buses being driven on the same routes they had been driven on January 22, 2020. They concluded that the outbreak on the two buses was due to long-range airborne transmission, although they did not investigate the possible contribution of fomite transmission.

Fig. 2 summarizes the journey timelines of the two buses. CCTV recordings had been made on the two buses at the time of the exposure event, but unfortunately these recordings were erased after the Hunan Provincial Center for Disease Control and Prevention had reviewed them in the early phase of their investigations (Ou et al., 2022). However, three screenshots of B1 recordings, four screenshots of B2 recordings, and the departure/arrival video clips of B2, were saved. These images were used to obtain data on passengers' mask wearing and other behaviors for the current study. Some of the screenshots are given as sketches for readers' comprehension (Figs. 3 and 4).

B1 departed from Changsha station at 12:10 and arrived at a southern town station (city D station) at 15:30 (Fig. 2a). The screenshots of the CCTV recordings from B1 (Fig. 3) and passengers' questionnaire

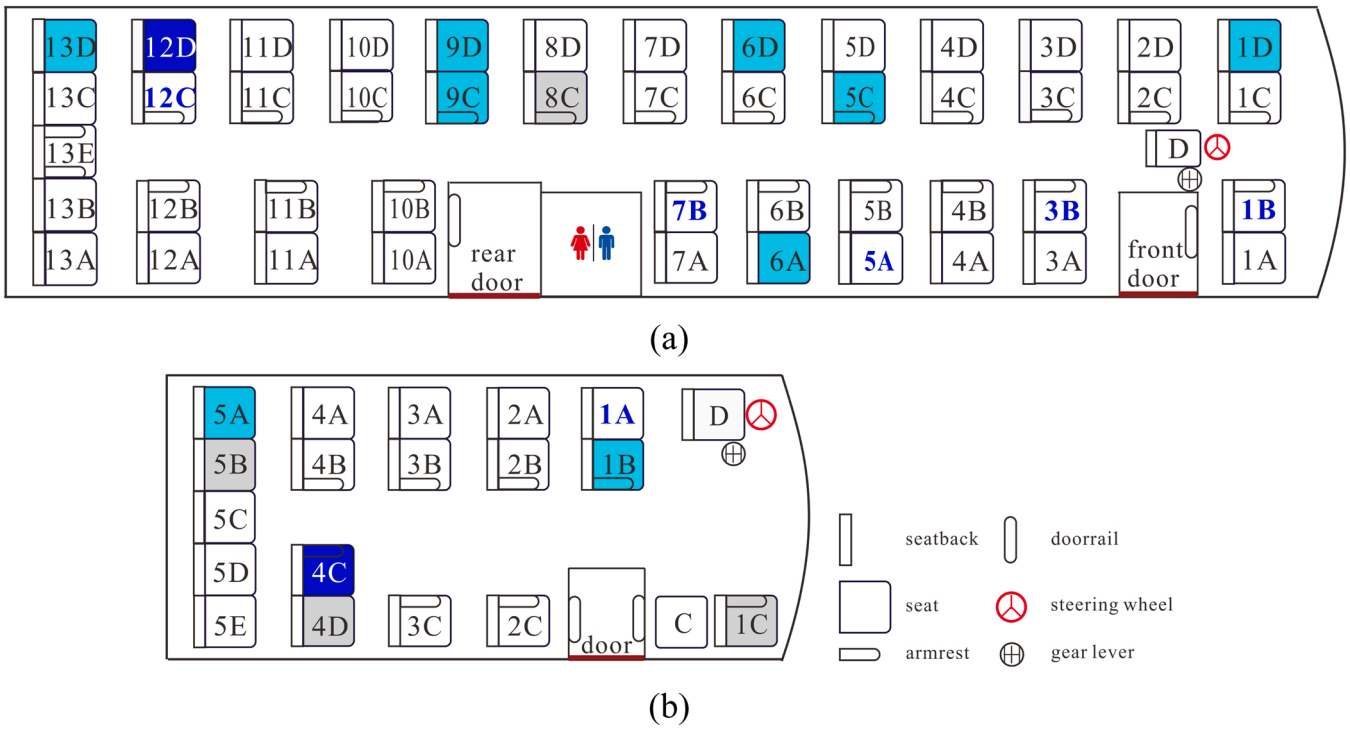

Fig. 1. Seating arrangements of the two buses involved in the Hunan two-bus COVID-19 outbreak. (a) B1, (b) B2. The seats on which the index case and infected cases sat are colored dark blue and light cyan, respectively; empty seats are colored gray. All of the seats are labeled by a unique number and letter combination, except for the seats of the driver and conductor, which are labeled as D and C, respectively. The seat labels of passengers who wore a face mask are colored dark blue and bolded.

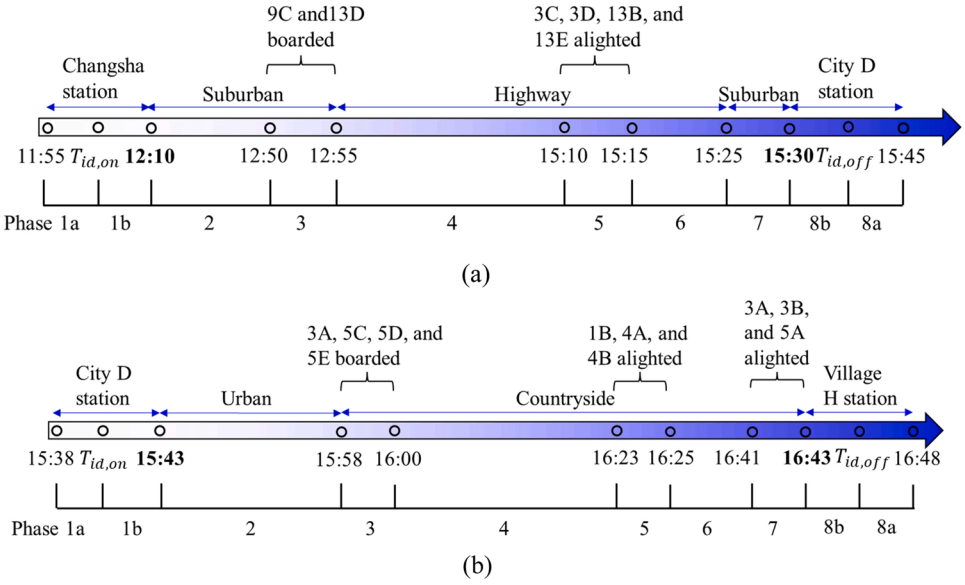

Fig. 2. The trip timelines of the two buses involved in the Hunan two-bus COVID-19 outbreak. The bus measured ventilation rate is affected by its speed, and each speed range is referred to as a phase. There are 8 phases (1–8) with two sub-phases in Phase 1 (i.e. 1a and 1b) and Phase 8 (i.e. 8a and 8b) each. The bus speed in each phase of the two buses is summarized in Table S1. (a) B1. Two 15-min time slots (11:55–12:10 and 15:30–15:45) were allocated before and after the journey, during which passengers boarded or alighted the bus. (b) B2. Two 5-min time slots (15:38–15:43 and 16:43–16:48) were allocated before and after the journey, during which passengers boarded or alighted the bus. Note that two 5-min time slots and three 2-min time slots were considered for passengers to board or alight B1 or B2, respectively, during the journeys of these buses (as the actual boarding and alighting durations during the journeys were unknown). Each phase is represented by a number or a number and letter combination. Each number marks a specific driving speed, bus location and ventilation rate. The letter "a" and "b" means that the index case was not on the bus and on the bus, respectively. $T_{id,on}$ and $T_{id,off}$ are the time when the index case boarded and alighted the bus, respectively. For details, please refer to Tables S1 and S2.

survey data show that two passengers (in seats 9C and 13D, respectively; hereafter, all passengers are referred to by their seat label) boarded B1 approximately 40–45 min into its trip, and four passengers (3C, 3D, 13B, and 13E) alighted approximately 16 km before city D station. For details, please refer to Tables S1 and S2.

B2 departed from city D station at 15:43 and arrived at village H station at 16:43 (Fig. 2b). The screenshots of the CCTV recordings from B2 (Fig. 4) and passengers' questionnaire survey data show that three passengers (3B, 3C, and 5A) boarded after the index case (4C) at city D station, and that four passengers (3A, 5C, 5D, and 5E) boarded later during the trip of B2, before 16:00. Four passengers (1B, 4A with a baby, and 4B) alighted approximately 15–20 min before the end of the trip,

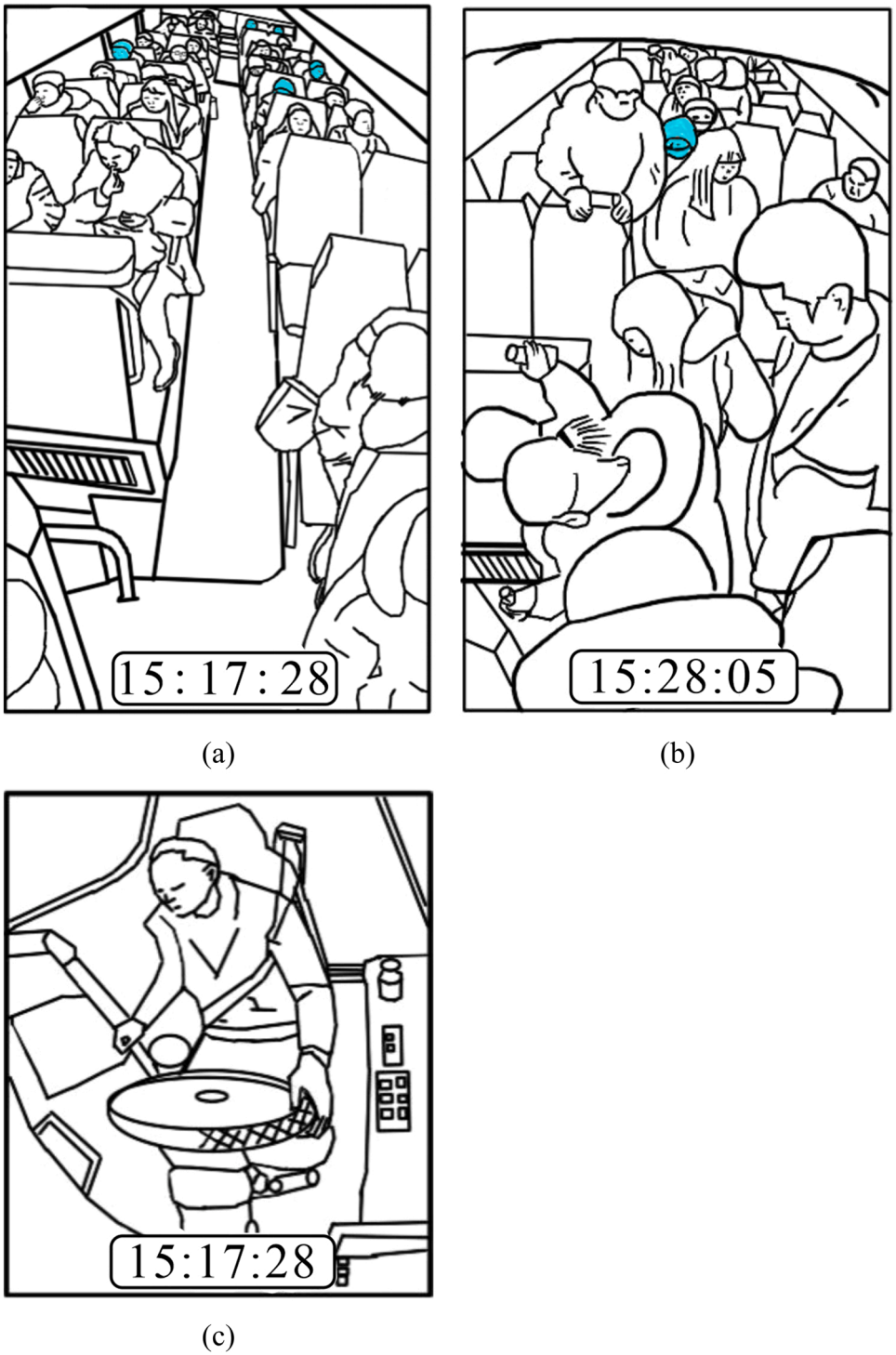

Fig. 3. Passenger and driver positions on B1. (a) Passenger positions and behaviors at 15:17:28. (b) Passenger positions and behaviors at 15:28:05. (c) Driver's behavior at 15:17:28.

and three passengers (3A, 3B, and 5A) alighted later, near village H station. For details, please refer to Tables S1 and S2.

2.2. Modeling framework

We first investigated the spatial characteristics of transmission by modeling a baseline scenario to estimate risk of the infection via fomite and airborne transmission on both buses. The index case did not show any symptoms, and did not talk with any passenger during the two bus journeys. We thus considered normal breathing (in through the nose and out through the mouth) (Morawska et al., 2009) as his only respiratory activity. We did not consider the child carried by his mother (passenger 4A) on B2 as he was exposed to a similar transmission risk as his mother. A least-squares fitting was performed to determine the probable values of the unknown parameters mentioned above and the dominant transmission route. Finally, the quanta generation rate of the index case on both buses was estimated. For the details of parameter values, please refer to Tables S3–S7.

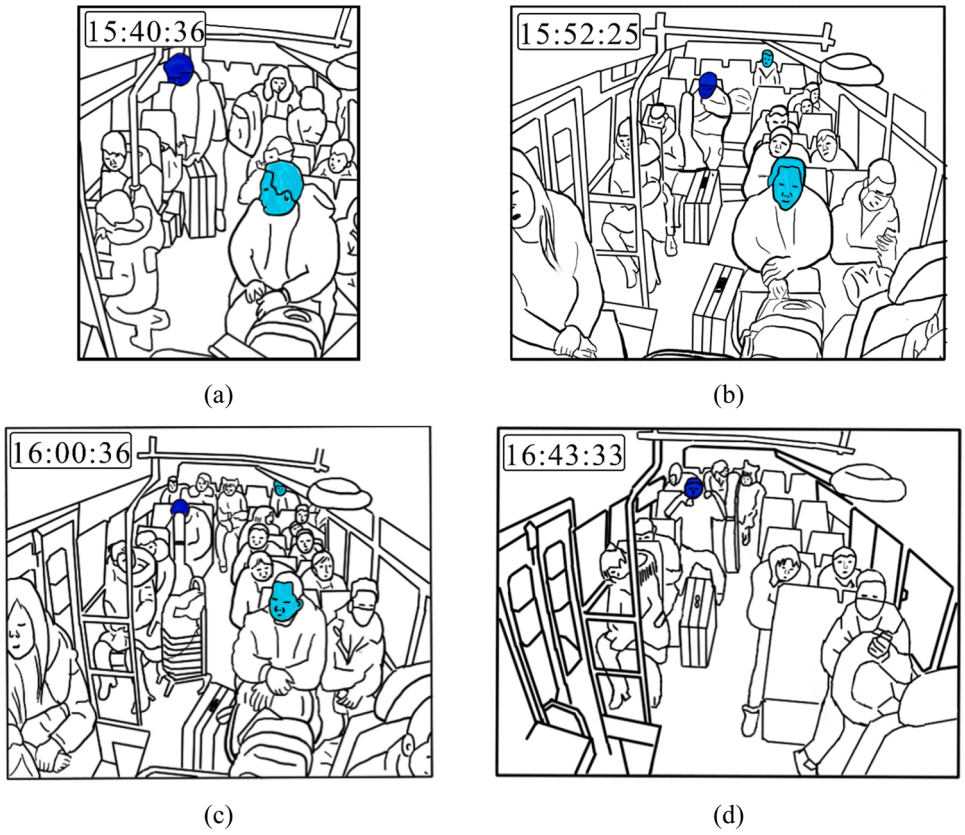

Fig. 4. Passenger arrangement on B2. (a) Passenger positions and behaviors at 15:40:36. (b) Passenger positions and behaviors at 15:52:25. (c) Passenger positions and behaviors at 16:00:36. (d) Passenger positions and behaviors at 16:43:33.

2.2.1. *Fomite transmission route*

People can self-inoculate by touching their mucous membranes after touching a contaminated object (fomite). We used the surface contamination model (Xiao et al., 2018a) to calculate the viral load on various fomites (environmental surfaces) and on passengers' hands and mucus membrane. The process by which viruses spread within a surface network was modeled as a discrete-time non-homogeneous Markov chain. Our Markov chain model was verified using data from two inflight norovirus outbreaks and from a small-scale benchtop experiment (Lei et al., 2017; Xiao et al., 2018c). Three kinds of touching behaviors were included in the fomite transmission route: touching the door rail and aisle seatbacks when boarding or alighting a bus; or touching surrounding surfaces (the back of the seat in front of a passenger's seat or the armrest of the passenger's or conductor's seat (if any), the steering wheel and gear lever (for the driver)) when seated; touching their own mucous membranes (e.g., eyes, nose, or mouth).

The total exposure dose of the *ith* individual via the fomite transmission route was calculated as follows:

$$D_f^i = \sum_{k=1}^{N_k} P_m^{i,k} C_h^{i,} \quad {}^k A_{cm}^i \alpha_{hm}^i \tag{1}$$

where N_k is the total number of time steps in each random simulation for each bus (920 on B1 and 280 on B2, with each time-step equals to 15 s, including boarding and alighting periods); $P_m^{i,k}$ is the indicator of the touching behavior of the *ith* individual in the k^{th} time step, which equals 1 if the individual touches his/her mucous membrane and equals 0 otherwise; $C_h^{i,k}$ is the virus concentration (RNA copies/cm^2) on the hand of the *ith* individual in the k^{th} time-step; A_{cm}^i is the contact area between the hand of the *ith* individual and his/her mucous membrane; and α_{hm}^i is the virus transfer rate from the hand of the *ith* individual to his/her mucous membrane.

2.2.2. *Airborne transmission route*

We combined the short-range and long-range airborne routes as the airborne route. Estimating the infection risk from airborne transmission required the determination of the total inhalation exposure of all passengers during the entire journey of each bus, for which at least two factors needed to be considered. First, the spatial distribution of expired aerosols, i.e. droplet nuclei of the fine expired droplets, is not uniform, although relatively good mixing is obtained for exhaled tracer gas in steady-state computational fluid dynamics (CFD) simulations (Ou et al., 2022). In Ou et al. (2022), most boundary conditions were obtained from the field experiments, and the predictions were validated by data from the field tracer gas experiment on the original two buses. Second, there can be significant temporal variation of infectious aerosols concentration on each bus. During their journey, each bus was driven through different phases characterized by different ventilation rates. Temporal changes were expected when one phase is switched to another phase. This was further complicated by the fact that the measured ventilation rate of a bus is affected by its speed (each speed range is referred to as a phase). There are 8 phases (1–8) with two sub-phases in Phase 1 (i.e. 1a and 1b) and Phase 8 (i.e. 8a and 8b) each. The bus speed, location, and window opening in each phase of the two buses are summarized in Table S1. Thus, transient CFD simulations of the passengers' and the driver's/conductor's inhalation exposures to exhaled droplets of different sizes on the two buses during their journeys would require prolonged computational time. We therefore used a simplified approach: we assumed that the spatial distribution of the expired aerosols would remain unchanged and equal that predicted by steady-state CFD in Ou et al. (2022).

We modeled the temporal effect using the classical macroscopic mass-balance equation model, which considers removal by ventilation,

virus deactivation, and deposition (Aganovic et al., 2021; Buonanno et al., 2020). The total exposure is thus estimated in four steps. First, the transient concentration $C(d_{md},t)$ for droplet nuclei of diameter d_{md} at time t on each of the two buses was determined using the macroscopic equation. Second, the ratio $R^i(t)$ of the droplet nuclei concentration at the mouth area of the i^{th} passenger at time t to that in the entire bus was estimated. Note that the ratio $R^i(t)$ is independent of droplet nuclei size. Third, the droplet nuclei concentration $C^i(d_{md},t)$ at the mouth area of the i^{th} passenger was calculated as the product of $C(d_{md},t)$ and $R^i(t)$. These first three steps are explained in the Supplementary materials S1.2. Finally, the total dose of exposure D_a^i of the i^{th} passenger via airborne transmission were evaluated as follows:

$$D_a^i = \sum_{md=1}^{4} \int_{t_{st}^i}^{t_{en}^i} C^i(d_{md},t)\cdot IR\cdot E_{md}\cdot \frac{1}{6}\pi d_{o,\ md}^3 \cdot \frac{L_o}{4}\cdot(1-\varphi)^{P_\varphi^i} \bullet \mathrm{dt} \quad (2)$$

where four different sizes (median diameter, or $md = 1$–4) of initially exhaled droplets were considered (0.8, 1.8, 3.5, and 5.5 μm; Morawska et al., 2009), t_{st} and t_{en} are the moments when the *ith* passenger boards and alights a bus, respectively; IR is the inhalation rate, which was assumed to be 0.49 m^3/h (Adams, 1993); E_{md} is the deposition efficiency of droplets of diameter d_{md} in the respiratory tract, as obtained from the International Commission on Radiological Protection (ICRP) deposition model (ICRP, 1994); L_o is the concentration of viral RNA in the initially exhaled droplets (which was set as 1×10^9 RNA copies/mL in the baseline scenario), which was divided by 4 as the number of viable viruses will decrease to 25% of its original value after full evaporation of the droplets (Xiao et al., 2018a); φ is the filtration efficiency of a face mask with ear loops (which was assumed to be 0.381 in this study (Sickbert-Bennett et al., 2020)); and P_φ^i is the indicator of whether the *ith* individual wears a mask, which equals 1 if he/she is wearing a mask and 0 otherwise. Note that we assumed a constant L_o for all droplet sizes.

2.3. Least-squares fitting

To avoid the effect on the simulation results brought by randomness, the simulation was conducted 1000 times for each bus. The predicted infection risk $P^{i,l}$ of the *ith* passenger in the *ith* simulation was calculated based on the dose–response relationship:

$$P^{i,l} = 1 - e^{-\eta_m D_f^{i,l} - \eta_r D_a^{i,l}} \quad (3)$$

where η_r and η_m are the dose–response parameters in the respiratory tract and mucous membrane, respectively, and $D_f^{i,l}$ and $D_a^{i,l}$ are D_f^i and D_a^i in the *ith* simulation, respectively. The transmission risk is denoted "to one" or ":1″ (decimals) in this paper.

Three viral load related parameters of SARS-CoV-2 transmission remain unknown, i.e. the initial virus concentration L_o in exhaled droplets and the dose–response parameters in the respiratory tract and mucous membrane, i.e., η_r and η_m, respectively. We adopted least-squares fitting to explore the probable values of these parameters and the dominant transmission route. To reduce the number of variables, we combined L_o, η_r and η_m as the effective inhalation viral load $\eta_r L_o$ and effective membrane viral load $\eta_m L_o$. Exhaled droplets of all sizes tend to have the same viral concentration (load), expressed as RNA copies per mL (Xiao et al., 2018a). Examining Eqs. (1)–(3), as the dose-response parameters η_r, η_m and the viral load L_o are constant, the effective inhalation viral load $\eta_r L_o$ and effective membrane viral load $\eta_m L_o$ can be determined if the infection risk is known as in the two-bus outbreak.

Following a lack of viral load data of the index case, we assigned a series of values (1×10^6–1×10^{11} RNA copies/mL), previously confirmed in patients on the day before or after symptom onset (e.g., Jones et al., 2021; Kim et al., 2020), to viral load L_o. η_r and η_m were assumed to be 1×10^{-1}–1×10^1 and 1×10^{-4}–1×10^{-2}, respectively, as in Xiao et al. (2018a), i.e., η_r was three orders of magnitude greater than η_m. We assigned 29 discrete values (increasing by $1 \times 10^{0.25}$) in the range of 1×10^5 –1×10^{12} to $\eta_r L_o$ and 17 discrete values in the range of 1×10^2 –1×10^9 to $\eta_m L_o$, and ensured that the ratio of $\eta_r L_o$ to $\eta_m L_o$ was in the range of 1×10^1 –1×10^5 (increasing by $1 \times 10^{0.25}$), which is the same as the ratio of η_r to η_m (Table S8). After eliminating some inappropriate scenarios, a total of 429 scenarios were considered in this study.

The residual sum of squares (RSS) for each scenario was averaged over 1000 simulations to estimate the fitness between the modeled infection risk and the reported attack rate, i.e., a smaller RSS represents a better fit.

$$RSS = \frac{1}{N_l} \sum_{l=1}^{N_l} \sum_{i=1}^{N_p} \left[I^i - P^{i,l}(\eta_r L_o,\ \eta_m L_o) \right]^2 \quad (4)$$

Where $1 \times 10^5 < \eta_r L_o < 1 \times 10^{12}$; $1 \times 10^2 < \eta_m L_o < 1 \times 10^9$; N_l is the number of random simulations (= 1000 in total); N_p is the number of passengers on each bus (excluding the index case); I^i is the infection indicator of each passenger (and equals 1 for an infected passenger and 0 for a non-infected passenger.

The values of the effective inhalation viral load $\eta_r L_o$ and effective membrane viral load $\eta_m L_o$ obtained for the best-fit scenario predict the viral load at the time of infection (Xiao et al., 2018a).

After having determined the best-fit scenario, i.e., the one with the minimum RSS, we compared the fomite transmission risk and airborne transmission risk of SARS-CoV-2. If transmission by the fomite route was negligible, this outbreak could be considered a case of airborne dominant transmission, and thus the quanta generation rate of the index case on each bus could be calculated.

2.4. Quanta generation rate

As in Section 2.3, we determined the best-fitting value of effective inhalation viral load $\eta_r L_o$ on each bus, which was used to estimate the quanta generation rate Q_i(quanta/h) of the index case on each bus.

$$Q_i = \sum_{md=1}^{4} E_{md}\cdot \frac{1}{6}\pi d_{o,\ md}^3 \bullet \eta_r L_o \Big/ 4\cdot N_{md} \bullet IR \quad (5)$$

Where md = 1–4 represents four sizes of the initially exhaled droplets as defined earlier; E_{md} is the deposition efficiency of droplets of diameter d_{md} (Table S3) in the respiratory tract, as obtained from the ICRP deposition model (ICRP, 1994); the effective inhalation viral load $\eta_r L_o$was determined by least-squares fitting, independent of droplet size, as 1.778×10^9/mL and 3.162×10^9/mL on B1 and B2, respectively; N_{md} is the number concentration of droplets with an initial diameter $d_{o,md}$ in the exhaled air; and IR is the exhalation flow rate (equals to inhalation flow rate) for a resting person (Adams, 1993), which was assumed to be 0.49 m^3/h. One quantum in the estimated quanta generation rate in this study can be understood as one viable SARS-CoV-2 virus that could deposit on susceptible individuals' respiratory tract and initiate infection.

3. Results

3.1. Spatial characteristics of predicted infection-risk patterns

The predicted infection risks via fomite transmission on both buses are presented in Fig. 5a and c. The overall infection risk via fomite transmission was negligible for many passengers on both buses. The aisle-seat passengers on both buses had a higher infection risk via fomite transmission than the window-seat passengers. This may be because passengers on the aisle side were in contact with contaminated armrests (non-porous surfaces), which transfer virus-containing droplets more efficiently to human hands than seatbacks (porous surfaces) (Xiao et al., 2018a). For example, passenger 13E on B1 could touch both armrests of

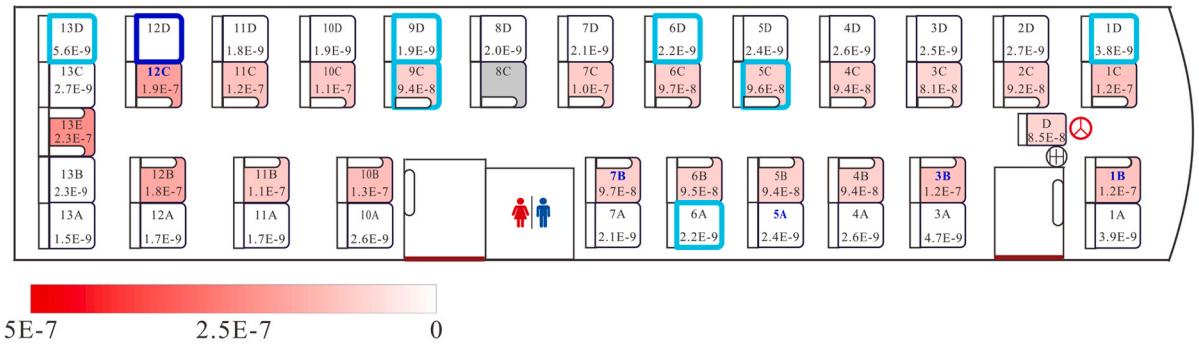

(a) Fomite transmission route

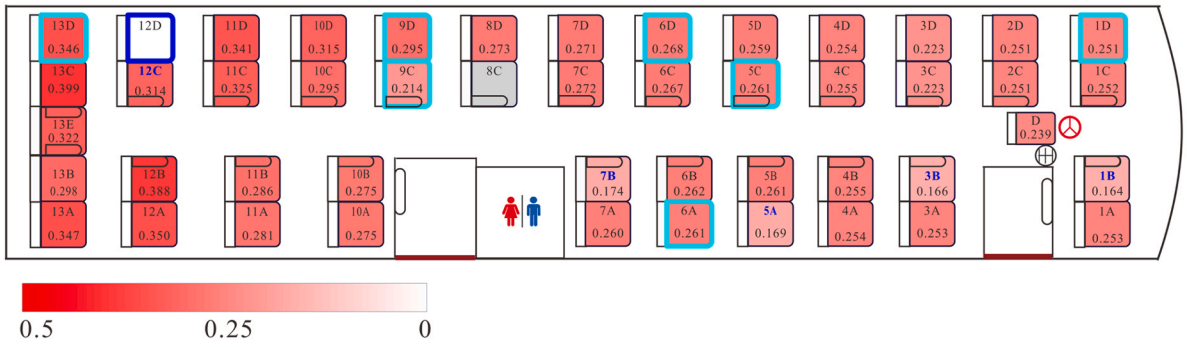

(b) Airborne transmission route

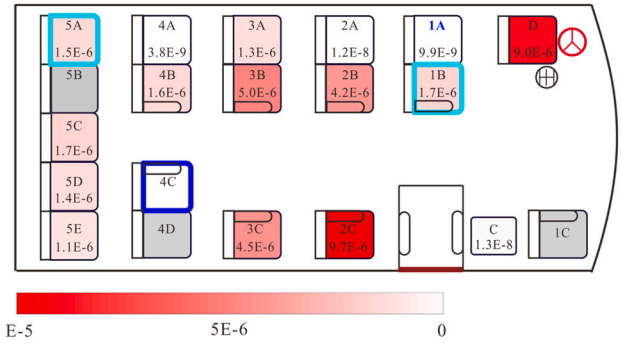

(c) Fomite transmission route

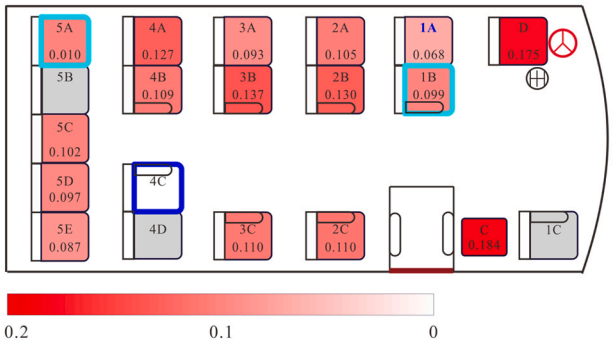

(d) Airborne transmission route

Fig. 5. Spatial distribution of the predicted average infection risk [in decimal, not percent] (for 1000 simulations) via fomite or airborne transmission at the end of the computational period. (a) Fomite transmission risk in B1, (b) airborne transmission risk in B1, (c) fomite transmission risk in B2, and (d) airborne transmission risk in B2. The dose–response parameters in the respiratory tract (η_r) = 3.2/RNA copy and that in the mucous membranes (η_m) = 3.2×10^{-3}/RNA copy, and the viral load (L_o) = 1×10^9 RNA copies/mL. Different levels of infection risk are represented by the intensity of red shading. Seats of the index case and the infected passengers are marked with thick dark blue and light cyan squares, respectively. There are two numbers in each seat square: the number at the top is the seat label, while that at the bottom is the simulated infection risk.

his/her seat, the non-porous surfaces of which could have transferred virus-containing droplets efficiently to his/her hands. Thus, passenger 13E was estimated to have a high infection risk via fomite transmission, even if the concentration of virus on the surfaces surrounding him/her was similar to that in droplets on surfaces surrounding his/her neighboring passengers (Fig. S1).

The predicted infection risks via airborne transmission on both buses are presented in Fig. 5b and d, where different color scales are used to denote the fomite and airborne transmission routes. The overall infection risk via the airborne route was much higher (approximately 1×10^6-fold to 1×10^8-fold higher) than that via the fomite route in the baseline scenarios. Unlike the fomite transmission route, the high infection risk via the airborne transmission route was not restricted to the aisle-seat passengers or to those near the index case, e.g., the driver and the conductor on B2. Moreover, passengers on these two buses faced different levels of infection risk via airborne transmission, owing to their different journey lengths and the different ventilation rates of the buses. This was also true for passengers on the same bus. For example, on B2, the virus concentrations in the mouth area of passengers 2B and 5C were quite similar (Fig. S1; Ou et al., 2022), but passenger 5C spent at least 15 min less than passenger 2B aboard B2, as passenger 2B boarded the bus after passenger 5C. Therefore, the infection risk of passenger 5C was lower than that of passenger 2B.

3.2. Predicted scenarios with the best fit

The RSS values for a total of 429 scenarios in each bus are shown in Figs. S2 and S3. On B1, there were 17 best-fit scenarios with the same RSS value of 5.994 and the effective inhalation viral load $\eta_r L_o$ value of 1.778×10^9. On B2, there were 14 best-fit scenarios with the same RSS value of 1.826 and the effective inhalation viral load $\eta_r L_o$ value of 3.162×10^9.

The most-likely scenario for each bus (the scenario with the highest the effective membrane viral load $\eta_m L_o$) is shown in Table 1. The predicted infection risks of passengers seated in different parts of each bus were closer to the reported attack rate in B1 than to that in B2. The differences between the observed and predicted infection risk in some parts of the two buses might be explained by the small sample size, errors in the human behavior data and other unknown factors. In addition, on both buses, the infection risk via airborne transmission was equal (to up to 3 decimal places) to that via multi-route transmission, whereas the infection risk via fomite transmission was almost 0, which highlights the predominance of the airborne transmission route and the insignificance of the fomite transmission route in this outbreak.

Table 1
Predicted scenarios with the best fit (the minimum RSS) for the two buses, and the observed data.

Parameter	B1		B2	
	Observed	Predicted	Observed	Predicted
Minimum RSS	N.A.	5.994	N.A.	1.826
$\eta_r L_o$(/mL)	Unknown	1.778×10^9	Unknown	3.162×10^9
$\eta_m L_o$(/mL)	Unknown	1.778×10^8[a]	Unknown	5.623×10^7[a]
Average infection risk [in decimal, not percent] (via both fomite and airborne routes)				
Adjacent seats[b]	0.000	0.210	0.000	0.098
Driver-side seats[b]	0.250	0.166	0.200	0.113
Non-driver-side seats[b]	0.050	0.156	0.000	0.117
Rear seats[b]	0.158	0.189	–	–
Front seats[b]	0.154	0.143	–	–
Aisle seats[b]	0.100	0.153	0.167	0.115
Non-aisle seats[b]	0.200	0.169	0.143	0.113
Overall	0.152	0.162	0.118	0.113
Overall infection risk via each route [in decimal, not percent] (all seats, including those of the driver/conductor)				
Fomite route	Unknown	3.154×10^{-6}	Unknown	4.688×10^{-5}
Airborne route	Unknown	0.162	Unknown	0.113

[a] There was more than one scenario with the best fit, and they all share the same $\eta_r L_o$ value. We chose to present the scenario with the largest $\eta_m L_o$ value.
[b] Please refer to Table S9 for seat classifications.

3.3. Predicted quanta generation rate of the index case on the two buses

The results shown in Section 3.2 reveal that the two-bus outbreak was predominantly an airborne transmission outbreak, as the contribution of fomite transmission in the best-fit scenarios was almost zero. The predicted quanta generation rate on B1 was 37.07 quanta/h, which is only 56% of that on B2 (65.92 quanta/h).

4. Discussion

4.1. Fomite transmission played a negligible role in the two-bus COVID-19 outbreak in Hunan

One of the most important findings of this modeling study of the two-bus COVID-19 outbreak in Hunan is that the fomite transmission route did not play a significant role in SARS-CoV-2 transmission. The predicted infection risk via the airborne transmission route was 0.162 (16.2%) on B1 and 0.113 (11.3%) on B2, whereas that via the fomite transmission route was only 3.154×10^{-6} (0.000315%) on B1 and 4.688×10^{-5} (0.00469%) on B2.

The settings on the two buses might offer some explanation for this difference: that is, the setting suggests that there were minimal interactions between passengers. This is particularly true for B1, which was traveling at a relatively high speed on a highway; none of its passengers left their seats during the entire journal, except during alighting, and no passenger used the on-board toilet. In addition, digital tickets were used on both buses, and thus passengers could only have had the opportunity to touch common surfaces while boarding or alighting. Furthermore, the index case did not show any symptoms during his journey, and he did not speak to anyone, and thus the only direct source of virus-laden droplets from this passenger would have been from normal breathing (with droplets in the range of 0.8–5.5 μm; Morawska et al., 2009). These small-sized droplets evaporate immediately after release, and have small nuclei; thus, there would have been only a low concentration of these nuclei deposited on any touchable surfaces (fomites) on the buses. This means it is probable that an insignificant number of viable viruses would have been present on only a small number of common surfaces.

Our results are in line with the general consensus on the fomite transmission of SARS-CoV-2 in the literature. Many environmental surface sampling studies have suggested that fomites and other surfaces in healthcare settings are not contaminated with viable SARS-CoV-2 (e.g., Chia et al., 2020; Colaneri et al., 2020). A commentary by Goldman (2020) suggested that the risk of fomite transmission was low, which was echoed by Mondelli et al. (2021). A recent modeling study also suggested that the risk of fomite transmission is low (Pitol and Julian, 2021).

Our modeling data for SARS-CoV-2 transmission in the two-bus outbreak are in contrast with the findings for a norovirus outbreak on a Boeing 747 airplane (Lei et al., 2017), in which the modeled fomite transmission risk was 25.6% (i.e., 0.256), while the reported infection risk was 33.6% (i.e., 0.336). In addition, the indoor settings also differ between our study and this previous study. In the airplane cabin, the toilet surfaces were contaminated, and some passengers visited the toilets during the 3-h flight, touching the aisle seatbacks on their way to and back from the toilet.

One interesting observation is that one passenger, 9D, who had no contact with the index case, became infected during the return trip of B1 from city D to Changsha, when the index case was not present (Ou et al., 2022). B1 stayed in city D for 30 min before starting its return trip to Changsha, and it remains unknown how passenger 9D became infected on this return trip. Notably, the passenger who sat in 9D on the first trip of B1 was also infected. If fomite transmission had caused the infection,

a few more passengers should have been infected on the return trip of B1, as no surface disinfection was conducted in B1 during its stop in city D. Thus, it would be useful to explore whether fomite transmission of SARS-CoV-2 via surface touch is possible for this case. Such transmission would require a larger exposure dose than that for airborne transmission, which is why we set such $\eta_m L_o << \eta_r L_o$ (Table S8). According to the steady-state CFD simulations, passengers on seats 9C/D, 10C/D, 11C/D are surrounded by a polluted air cloud with the second highest tracer gas concentration (see Fig. 3 in Ou et al., 2022). The seat and other nearby surfaces might have been contaminated by the deposited aerosols.

Importantly, virus particles deposited on a fomite can be resuspended, i.e., become airborne. Licina and Nazaroff (2018) showed that up to 3% of the deposited particles on cloth were subsequently released with fabric motion. Qian and Ferro (2008) showed how feet tapping can lead to resuspension. Accordingly, we speculate that the action of sitting on a seat can also lead to the release of viral particles from the seat into the air. Some studies have suggested that fomites in cold-chain transport might also lead to transmission (e.g., Ji et al., 2021). Our speculated fomite-resuspension mechanism warrants further in-depth study to verify the possible roles of contaminated fomites in the spread of SARS-CoV-2.

4.2. Predominance of airborne transmission

The second major finding of this study is that airborne transmission was the predominant route of virus transmission in the two-bus outbreak. The significance of airborne transmission of SARS-CoV-2 has now been widely recognized (e.g., Miller et al., 2021). In fact, one of the authors (Li) has presented the data of this Hunan two-bus outbreak (including detailed data on ventilation rates) at various international workshops since mid-2020, including those organized by the WHO. Notably, this is one of the very few SARS-CoV-2 outbreaks for which detailed data were available on the ventilation of infection venues. During the past decades, airborne transmission has been shown to be an important transmission route for SARS-CoV-1 in indoor environments (Li et al., 2005; Yu et al., 2004). Thus, considering the similarities between SARS-CoV-1 and SARS-CoV-2 (Yan et al., 2020), it is likely that airborne transmission plays the leading role in COVID-19 spread.

The unique aspect of this Hunan bus outbreak is that two infection venues were involved in the same outbreak: to our knowledge, no other multi-venue outbreak involving a single index case has been reported. Our findings regarding this outbreak have significant implications. If we assume that the expired source strength of the virus from the index case was the same on both buses, it is intriguing that each bus had a different attack rate. This may be related to the fact that the time-averaged ventilation rates were 1.72 L/s per person on B1 and 3.22 L/s per person on B2, both of which are lower than the recommended 8–10 L/s per person for offices and other indoor settings (e.g., American Society of Heating Refrigerating and Air-Conditioning Engineers (ASHRAE), 2019). Thus, the observed attack rates were 0.152 (or 15.2%) on B1 and 0.118 (or 11.8%) on B2, and the predicted attack rates due to airborne transmission were 0.162 (or 16.2%) on B1 and 0.113 (or 11.3%) on B2. The predicted attack rates are very similar to the corresponding observed attack rates, and the higher ventilation rate on B2 corresponds to the lower attack rate on B2 than on B1. Note that the air flows on the two buses were reasonably mixed but not fully mixed (Ou et al., 2022), and that air flow patterns are known to affect rates of infection (Qian and Zheng, 2018).

The so-called best-fit scenarios on both buses warrant discussion. In the predicted best-fit scenario, the effective inhalation viral load $\eta_r L_o$ on B1 was 1.778×10^9, while that on B2 was 3.162×10^9. Thus, the effective inhalation viral load $\eta_r L_o$ for the best-fit scenario on B2 was 1.8 times that on B1, suggesting that the viral load on B2 was higher than that on B1. This trend agrees with the estimated infectious quanta generation rates on the two buses (35.0 h^{-1} on B1 and 58.3 h^{-1} on B2) reported by Ou et al. (2022) under a steady-state assumption, with the quanta generation rate on B2 being 1.7 times that on B1. Both the quanta estimate by Ou et al. (2022) and our new best-fit scenario estimate revealed that there was a larger viral load released on B2 than on B1. This is attributable to the fact that there can be significant variations in the SARS-CoV-2 load of droplets expired by the same person over a 4–6-h period, as the peak-load period is around the time of symptom onset (e.g., Jones et al., 2021; Kim et al., 2020).

The video clip of B2 departing revealed that while the index case was waiting in the aisle to sit, two passengers (who appeared to be a young mother with a 5–7-year-old girl, who had been passengers on an earlier journey of B2) who had been sitting on seats at the back walked past the index case and then alighted the bus. The mother and the index case had a few seconds of face-to-face close contact during this movement, but neither she nor the young girl became infected.

4.3. Implications for infection control and further studies

This modeling study has revealed the predominance of airborne transmission and the insignificance of fomite transmission in the two-bus COVID-19 outbreak in Hunan. This is the second outbreak for which data were available on human behavior at the time of infection, together with detailed data on the environmental conditions at the infection venue. The first such COVID-19 outbreak for which detailed data were available occurred in a restaurant in Guangzhou in early 2020, and has been studied by Li et al. (2021b) and Zhang et al. (2021). The conclusions of these studies were similar to our own conclusion regarding the relative importance of airborne and fomite routes of transmission, except for one key difference. In the Guangzhou restaurant outbreak, the measured ventilation rate was approximately 1 L/s per person, whereas in the two-bus outbreak, the measured ventilation rates were higher (1.7 L/s per person and 3.2 L/s per person). Thus, our study shows that a ventilation rate of 3.2 L/s per person is insufficient to control SARS-CoV-2 transmission between people at rest.

This study is also the first to reveal that the release rate of infectious aerosols from the same pre-symptomatic index case can vary over a 5-h period. For instance, the release rate of infectious aerosols from the index case varied significantly between the first 3-h-20-min trip and the subsequent 1-h trip, despite the time between these trips being less than 15 min. Thus, the source strength differed for this same index case over a single afternoon. The Wells–Riley equation or its variants may be used for estimating threshold ventilation rates. Such an approach is only meaningful if all possible infectious quanta generation rates are known for a given scenario. Further studies of temporal variations in infectious quanta generation rates are needed. Note that temporal variations in infectious quanta generation rate do not track with temporal variations in viral load (Jones et al., 2021; Kim et al., 2020), as a viral load profile is not indicative of infectiousness.

Although the typical route of fomite transmission (that initiated by a hand touching a fomite bearing droplets containing virus) might not play a significant role in virus transmission, the resuspension of virus-laden droplets deposited on fomites creates virus-laden aerosols that can lead to airborne transmission. We thus hypothesize that the resuspension of virus-laden droplets from fomites might contribute to the transmission of respiratory viruses such as SARS-CoV-2. Further research is warranted to gather evidence to support or refute this hypothesis.

4.4. Limitations

Our study has several major limitations. First, the sample size in the two-bus outbreak was small, as it included only 10 infected passengers: 7 of the 46 passengers on B1, 1 passenger on the return trip of B1 (when the index case was not present), and 2 of the 16 passengers on B2. We speculate that the analysis of ventilation and human behavior data for a much larger outbreak (should these data become available) would yield

a more meaningful predicted viral load in a best-fit scenario than that we obtained in the current study.

Second, the human behavior data we used might deviate from real data, as complete CCTV recordings of the infection event were not available. Thus, the boarding and alighting times of most passengers were unknown, and had to be randomly assigned, as did passengers' surface-touching frequency. Most human behavior data were obtained from the re-collection performed by Hunan CDC staff who had reviewed the full CCTV recordings, and the remaining data were obtained from three screenshots of B1 recordings, four screenshots of B2 recordings, video clips of the departure/arrival of B2, and a questionnaire survey answered by some of the passengers. Fortunately, our engineering team was able to measure the ventilation rates in the two buses as these buses were being driven on the same routes (by the same drivers) they had taken on the day of the outbreak, before these buses were sold by the bus company. Our engineering team was not involved in the initial epidemiological study of this outbreak. It is recommended that an engineering team is involved in any future outbreak investigations.

Third, our methodology has several shortcomings. For example, we integrated the macroscopic mass-balance equation model with steady-state CFD simulated data to account for the non-uniform distribution of virus-laden droplets in the bus cabin, by using an instantaneous distribution from the steady state CFD simulation to represent any change in conditions. In addition, we assumed there was a constant ventilation rate in each phase of the trip (in reality, the ventilation rate changes according to bus speed and wind direction). Moreover, we used droplet-release data from the literature for the index case; however, there is known to be significant inter-individual variability in droplet release. Finally, we also assumed that there was an identical viral concentration in all droplets, irrespective of their size. More efforts to collect input data for outbreak modeling are warranted as such modeling can provide useful insights into several epidemiological factors, as demonstrated in our study.

5. Conclusion

We modeled SARS-CoV-2 transmission that occurred during the two-bus COVID-19 outbreak in Hunan, China, in January 2020. Our results show that airborne transmission was predominant in this outbreak, whereas fomite transmission was negligible. A ventilation rate of 3.2 L/s per person was found to be insufficient to prevent infection, suggesting that the threshold ventilation rate for the minimization of SARS-CoV-2 transmission is greater than 3.2 L/s per person. We found that the release rate of infectious aerosols from the single pre-symptomatic index case in the two bus trips varied over a 5-h period, indicating that the source strength differed significantly in the index case over this short period. This suggests the need for further studies of temporal variations in the infectious quanta generation rate of SARS-CoV-2. Notably, it remains unknown how a passenger became infected on the return trip of one of the buses when the index case was not present. Although we found that the fomite route (via surface touch) made an insignificant contribution to SARS-CoV-2 transmission during this two-bus outbreak, our hypothesis that the resuspension of virus-laden droplets from fomites may contribute to airborne transmission warrants further exploration.

CRediT authorship contribution statement

Pan Cheng, Kaiwei Luo, Shenglan Xiao: Conceptualization, Methodology, Software, Investigation, Formal analysis, Data curation, Visualization, Writing – original draft, Writing – review & editing. **Hongyu Yang, Jian Hang, Cuiyun Ou:** Investigation, Writing – review & editing. **Benjamin J Cowling, Hui-Ling Yen, David SC Hui, Shixiong Hu:** Visualization, Writing – review & editing. **Yuguo Li:** Conceptualization, Methodology, Formal analysis, Writing – review & editing, Supervision, Project administration, Funding acquisition.

Declaration of Competing Interest

The authors declare that they have no known competing financial interests or personal relationships that could have appeared to influence the work reported in this paper.

Acknowledgment

This work was supported by the Health and Medical Research Fund Commissioned Research on the Novel Coronavirus Disease (COVID-19) [Grant no. COVID190113], Hong Kong SAR, China.

Appendix A. Supporting information

Supplementary data associated with this article can be found in the online version at doi:10.1016/j.jhazmat.2021.128051.

References

Adams, W.C., 1993. Measurement of Breathing Rate and Volume in Routinely Performed Daily Activities. Final Report. Human Performance Laboratory, Physical Education Department, University of California, Davis. Human Performance Laboratory, Physical Education Department, University of California, Davis. Prepared for the California Air Resources Board, Contract No. A033-205, April 1993.

Atkinson, M.P., Wein, L.M., 2008. Quantifying the routes of transmission for pandemic influenza. Bull. Math. Biol. 70 (3), 820–867.

American Society of Heating Refrigerating and Air-Conditioning Engineers (ASHRAE), 2019. Ventilation for Acceptable Indoor Air Quality, ANSI/ASHRAE Standard 62.1-2019. Atlanta, USA.

Aganovic, A., Bi, Y., Cao, G., Drangsholt, F., Kurnitski, J., Wargocki, P., 2021. Estimating the impact of indoor relative humidity on SARS-CoV-2 airborne transmission risk using a new modification of the Wells-Riley model. Build. Environ. 205, 108278.

Bae, S., Kim, H., Jung, T.Y., Lim, J.A., Jo, D.H., Kang, G.S., Jeong, S.H., Choi, D.K., Kim, H.J., Cheon, Y.H., Chun, M.K., Kim, M., Choi, S., Chun, C., Shin, S.H., Kim, H. K., Park, Y.J., Park, O., Kwon, H.J., 2020. Epidemiological characteristics of COVID-19 outbreak at fitness centers in Cheonan, Korea. J. Korean Med. Sci. 35 (31), e288.

Buonanno, G., Morawska, L., Stabile, L., 2020. Quantitative assessment of the risk of airborne transmission of SARS-CoV-2 infection: prospective and retrospective applications. Environ. Int. 145, 106112.

Bogoch, I.I., Watts, A., Thomas-Bachli, A., Huber, C., Kraemer, M.U., Khan, K., 2020. Pneumonia of unknown aetiology in Wuhan, China: potential for international spread via commercial air travel. J. Travel Med. 27 (2), taaa008.

Charlotte, N., 2020. High rate of SARS-CoV-2 transmission due to choir practice in France at the beginning of the COVID-19 pandemic. J. Voice. ⟨https://doi.org/10.1016/j.jvoice.2020.11.029⟩, (In press).

Chia, P.Y., Coleman, K.K., Tan, Y.K., Ong, S.W.X., Gum, M., Lau, S.K., Marimuthu, K., et al., 2020. Detection of air and surface contamination by SARS-CoV-2 in hospital rooms of infected patients. Nat. Commun. 11 (1), 1–7.

Chin, A.W., Chu, J.T., Perera, M.R., Hui, K.P., Yen, H.L., Chan, M.C., Peiris, M., Poon, L. L., 2020. Stability of SARS-CoV-2 in different environmental conditions. Lancet Microbe 1 (1), e10.

Colaneri, M., Seminari, E., Novati, S., Asperges, E., Biscarini, S., Piralla, A., Percivalle, E., Cassaniti, I., Baldanti, F., Bruno, R., Mondelli, M.U., The COVID19 IRCCS San Matteo Pavia Task Force, 2020. Severe acute respiratory syndrome coronavirus 2 RNA contamination of inanimate surfaces and virus viability in a health care emergency unit. Clin. Microbiol. Infect. 26 (8), 1094.e1–1094.e5 e1-1094.e5.

Goldman, E., 2020. Exaggerated risk of transmission of COVID-19 by fomites. Lancet Infect. Dis. 20 (8), 892–893.

ICRP, 1994. Human respiratory tract model for radiological protection. A report of a Task Group of the International Commission on Radiological Protection. Ann. ICRP 24 (1–3), 1–482.

Jones, T.C., Biele, G., Mühlemann, B., Veith, T., Schneider, J., Beheim-Schwarzbach, J., Bleicker, T., Tesch, J., Schmidt, M.L., Sander, L.E., Kurth, F., Menzel, P., Schwarzer, R., Zuchowski, M., Hofmann, J., Krumbholz, A., Stein, A., Edelmann, A., Corman, V.M., Drosten, C., 2021. Estimating infectiousness throughout SARS-CoV-2 infection course. Science 373 (6551), eabi5273.

Ji, W., Li, X., Chen, S., Ren, L., 2021. Transmission of SARS-CoV-2 via fomite, especially cold chain, should not be ignored. Proc. Natl. Acad. Sci. USA 118 (11), e2026093118.

Kim, S.E., Jeong, H.S., Yu, Y., Shin, S.U., Kim, S., Oh, T.H., Park, K.H., et al., 2020. Viral kinetics of SARS-CoV-2 in asymptomatic carriers and presymptomatic patients. Int. J. Infect. Dis. 95, 441–443.

Lei, H., Li, Y., Xiao, S., Yang, X., Lin, C., Norris, S.L., Ji, S., et al., 2017. Logistic growth of a surface contamination network and its role in disease spread. Sci. Rep. 7 (1), 1–10.

Li, Y., Huang, X., Yu, I.T.S., Wong, T.W., Qian, H., 2005. Role of air distribution in SARS transmission during the largest nosocomial outbreak in Hong Kong. Indoor Air 15 (2), 83–95.

Li, Y., Cheng, P., Qian, H., 2021a. Dominant transmission route of SARS-CoV-2 and its implication to indoor environment. Kexue Tongbao/Chin. Sci. Bull. 417–423.

Li, Y., Qian, H., Hang, J., Chen, X., Cheng, P., Ling, H., Wang, S., Liang, P., Li, J., Xiao, S., Wei, J., Liu, L., Cowling, B.J., Kang, M., 2021b. Probable airborne transmission of SARS-CoV-2 in a poorly ventilated restaurant. Build. Environ. 196, 107788.
Licina, D., Nazaroff, W.W., 2018. Clothing as a transport vector for airborne particles: chamber study. Indoor Air 28 (3), 404–414.
Morawska, L.J.G.R., Johnson, G.R., Ristovski, Z.D., Hargreaves, M., Mengersen, K., Corbett, S., Katoshevski, D., et al., 2009. Size distribution and sites of origin of droplets expelled from the human respiratory tract during expiratory activities. J. Aerosol Sci. 40 (3), 256–269.
Morawska, L., Cao, J., 2020. Airborne transmission of SARS-CoV-2: the world should face the reality. Environ. Int. 139, 105730.
Meselson, M., 2020. Droplets and aerosols in the transmission of SARS-CoV-2. N. Engl. J. Med. 382 (21), 2063. -2063.
Miller, S.L., Nazaroff, W.W., Jimenez, J.L., Boerstra, A., Buonanno, G., Dancer, S.J., Noakes, C., et al., 2021. Transmission of SARS-CoV-2 by inhalation of respiratory aerosol in the Skagit Valley Chorale superspreading event. Indoor Air 31 (2), 314–323.
Mondelli, M.U., Colaneri, M., Seminari, E.M., Baldanti, F., Bruno, R., 2021. Low risk of SARS-CoV-2 transmission by fomites in real-life conditions. Lancet Infect. Dis. 21 (5), e112.
Oztig, L.I., Askin, O.E., 2020. Human mobility and coronavirus disease 2019 (COVID-19): a negative binomial regression analysis. Public Health 185, 364–367.
Oran, D.P., Topol, E.J., 2021. The proportion of SARS-CoV-2 infections that are asymptomatic: a systematic review. Ann. Intern. Med. 174 (5), 655–662.
Ou, C., Hu, S., Luo, K., Yang, H., Hang, J., Cheng, P., Hai, Z., Xiao, S., Qian, H., Xiao, S., Jing, X., Xie, Z., Ling, H., Liu, L., Gao, L., Deng, Q., Cowling, B.J., Li, Y., 2022. Insufficient ventilation led to a probable long-range airborne transmission of SARS-CoV-2 on two buses. Build. Environ. 207 (Part A), 108414.
Pitol, A.K., Julian, T.R., 2021. Community transmission of SARS-CoV-2 by surfaces: risks and risk reduction strategies. Environ. Sci. Technol. Lett. 8 (3), 263–269.
Qian, J., Ferro, A.R., 2008. Resuspension of dust particles in a chamber and associated environmental factors. Aerosol Sci. Technol. 42 (7), 566–578.
Qian, H., Zheng, X., 2018. Ventilation control for airborne transmission of human exhaled bio-aerosols in buildings. J. Thorac. Dis. 10 (Suppl. 19), S2295.
Sia, S.F., Yan, L.M., Chin, A.W., Fung, K., Choy, K.T., Wong, A.Y., Peiris, M., et al., 2020. Pathogenesis and transmission of SARS-CoV-2 in golden hamsters. Nature 583 (7818), 834–838.
Sickbert-Bennett, E.E., Samet, J.M., Clapp, P.W., Chen, H., Berntsen, J., Zeman, K.L., Bennett, W.D., et al., 2020. Filtration efficiency of hospital face mask alternatives available for use during the COVID-19 pandemic. JAMA Intern. Med. 180 (12), 1607–1612.
US CDC, 2021. Science brief: SARS-CoV-2 and surface (fomite) transmission for indoor community environments. Updated April 5, 2021. ⟨https://www.cdc.gov/coronavirus/2019-ncov/more/science-and-research/surface-transmission.html⟩. (Accessed 19 September 2021).
Van Doremalen, N., Bushmaker, T., Morris, D.H., Holbrook, M.G., Gamble, A., Williamson, B.N., Lloyd-Smith, J.O., et al., 2020. Aerosol and surface stability of SARS-CoV-2 as compared with SARS-CoV-1. N. Engl. J. Med. 382 (16), 1564–1567.
World Health Organization, 2020a. Modes of Transmission of Virus Causing COVID-19: Implications for IPC Precaution Recommendations: Scientific Brief, 29 March 2020. World Health Organization. ⟨https://apps.who.int/iris/handle/10665/331616⟩. (Accessed 9 October 2021).
World Health Organization, 2020b. Transmission of SARS-CoV-2: Implications for Infection Prevention Precautions: Scientific Brief, 09 July 2020. World Health Organization. ⟨https://apps.who.int/iris/handle/10665/333114⟩. (Accessed 9 October 2021).
Xiao, S., Li, Y., Wong, T.W., Hui, D.S., 2017. Role of fomites in SARS transmission during the largest hospital outbreak in Hong Kong. PLoS One 12 (7), e0181558.
Xiao, S., Li, Y., Sung, M., Wei, J., Yang, Z., 2018a. A study of the probable transmission routes of MERS-CoV during the first hospital outbreak in the Republic of Korea. Indoor Air 28 (1), 51–63.
Xiao, S., Tang, J.W., Hui, D.S., Lei, H., Yu, H., Li, Y., 2018b. Probable transmission routes of the influenza virus in a nosocomial outbreak. Epidemiol. Infect. 146 (9), 1114–1122.
Xiao, S., Li, Y., Lei, H., Lin, C.H., Norris, S.L., Yang, X., Zhao, P., 2018c. Characterizing dynamic transmission of contaminants on a surface touch network. Build. Environ. 129, 107–116.
Yu, I.T., Li, Y., Wong, T.W., Tam, W., Chan, A.T., Lee, J.H., Ho, T., et al., 2004. Evidence of airborne transmission of the severe acute respiratory syndrome virus. N. Engl. J. Med. 350 (17), 1731–1739.
Yan, Y., Chang, L., Wang, L., 2020. Laboratory testing of SARS-CoV, MERS-CoV, and SARS-CoV-2 (2019–nCoV): current status, challenges, and countermeasures. Rev. Med. Virol. 30 (3), e2106.
Zheng, R., Xu, Y., Wang, W., Ning, G., Bi, Y., 2020. Spatial transmission of COVID-19 via public and private transportation in China. Travel Med. Infect. Dis. 34, 101626.
Zhao, S., Zhuang, Z., Ran, J., Lin, J., Yang, G., Yang, L., He, D., 2020. The association between domestic train transportation and novel coronavirus (2019-nCoV) outbreak in China from 2019 to 2020: a data-driven correlational report. Travel Med. Infect. Dis. 33, 101568.
Zhang, N., Chen, X., Jia, W., Jin, T., Xiao, S., Chen, W., Kang, M., et al., 2021. Evidence for lack of transmission by close contact and surface touch in a restaurant outbreak of COVID-19. J. Infect. 83 (2), 207–216.